Supporting Information

Monoclinic oxygen-deficient tungsten oxide nanowires for the dynamic and independent control of near-infrared and visible light transmittance

Shengliang Zhang,[a,b] Sheng Cao,[a,b] Tianran Zhang,[a,b] Qiaofeng Yao,[a] Adrian Fisher[b,c] and Jim Yang Lee*[a,b]

[a] Department of Chemical and Biomolecular Engineering, National University of Singapore, 10 Kent Ridge Crescent, Singapore 119260, Singapore. Email: cheleejy@nus.edu.sg

[b] Cambridge Centre for Advanced Research and Education in Singapore, 1 Create Way, 138602, Singapore.

[c] Department of Chemical Engineering and Biotechnology, University of Cambridge, Pembroke Street, Cambridge CB2 3RA, United Kingdom.

Experimental

Materials

Ammonium metatungstate hydrate (AMT, $(NH_4)_6H_2W_{12}O_{40}).xH_2O$, 99.99%), oleylamine (>98%), toluene (anhydrous, 99.8%), N,N-dimethylformamide (DMF, anhydrous, 99.8%), isopropanol (IPA,>98%), lithium bis(trifluoromethanesulfonyl) imide (Li-TFSI, 99.95 wt%), Tetramethylammonium bis(trifluoromethanesulfonyl)imide (TBA-TFSI, 97%), tetraglyme (>99%), propylene carbonate (PC, anhydrous, 99.7%), tetrachloroethylene (TCE, anhydrous, >99%) and Hellmanex III cleaning solution were purchased from Sigma-Aldrich. All chemicals were used as received. ITO glasses (2 cm × 2 cm, 20 Ω sq^{-1}) were supplied by Latech.

Synthesis of $W_{18}O_{49}$ nanowires (NWs)

0.1 mmol AMT and 20 mL oleylamine were added to a 50 mL three-neck flask. After 10 min of vacuum degassing at 120 °C, the mixture was heated quickly to 250 °C in N_2 and kept at

this temperature for 2 h. After cooling to room temperature, the product was precipitated with excess ethanol, centrifugally separated (10000 rpm, 10 min) and then redispersed in toluene. Centrifugation and toluene washing were repeated once before the $W_{18}O_{49}$ NWs were finally dispersed in toluene to a concentration of ~60 mg mL^{-1}.

Preparation of monoclinic WO_{3-x} NW films

The 2 cm × 2 cm ITO glasses (20 Ω sq^{-1}) were first thoroughly cleaned with 2 vol % Hellmanex III solution for 15 min, rinsed with deionized water, and then washed with acetone and isopropanol (IPA) for 15 min each. 100 μL of the $W_{18}O_{49}$ NW solution (~60 mg mL^{-1}) was then spin-coated on a ITO glass at 1000 rpm for 60 s. Spin-coating was repeated 4 times to build up the film thickness. The as-deposited $W_{18}O_{49}$ NW film on ITO glass was then heat treated in air at 400 °C for 50 min (2 ℃/min) to remove the organic ligands. A transparent monoclinic WO_{3-x} NW film on ITO was produced. For the preparation of the bulk WO_3 films on ITO glasses, 100 μL AMT solution (400 mg mL^{-1}, dispersed in DMF) was spin-coated 2 times on an ITO glass at 1000 rpm for 30 s first, and then at 2000 rpm for 30 s. Thereafter the film was heat treated in air at 400°C for 1 h to form a bulk monoclinic WO_3 film on ITO, and at 350 °C for 1 h to form a bulk amorphous WO_3 (bulk a-WO_3) film on ITO.

Materials Characterization

The morphology of $W_{18}O_{49}$ NWs were examined by transmission electron microscopy (TEM) on a JEOL 2100F operating at 200 kV. X-ray diffraction (XRD) patterns were recorded by a Bruker D8 advance X-ray diffractometer using the Cu Kα radiation (1.5405Å). The changes of crystal structure in the process of phase transitions were identified by ex situ XRD using samples which had been conditioned at the potentials of interest for 2 h. X-ray photoelectron spectroscopy (XPS) analysis was carried out on a Kratos AXIS Ultra DLD surface analyzer using a monochromatic Al Ka radiation source at 15 kV (1486.71 eV). A JEOLJSM-6700F

field emission scanning electron microscope (FESEM) was used to inspect the deposited film morphology, and to determine the film thickness from cross-sectional SEM images. Optical transmittance/absorbance spectra were collected from a ASD LabSpec 4 VIS/NIR spectrometer. The surface roughness of films was characterized by atomic force microscopy (AFM, Bruker) operating in the tapping mode. Nitrogen adsorption measurements were performed at 77 K using a Quantachrome Autosorb gas-sorption system.

Electrochemical and electrochromic measurements

All electrochemical and electrochromic measurements were carried out in an argon glove box, using a custom-made spectroelectrochemical cell in the three-electrode configuration. The spectrometer was connected to the light source by fiber-optics. Prior to cell assembly, a coated ITO glass was dried in a vacuum oven at 60 °C for overnight and then used as the working electrode. For standard Li^+ intercalation/de-intercalation measurements, the counter and the reference electrodes were Li foils and the electrolyte was 0.5 M Li-TFSI in tetraglyme. For the purely capacitive charging measurements, a Pt foil counter electrode was used together with a Ag/Ag^+ reference electrode (in 0.1 M TBA-TFSI/PC) and a 0.1 M TBA-TFSI in PC electrolyte. All the potentials were calibrated against a Li foil reference electrode. Chronoamperometry (CA) and cyclic voltammetry (CV) were performed on an Autolab electrochemical workstation. CV was typically scanned between 4-2 V vs Li^+/Li at 2 mV s^{-1}. The scan rate was increased to 20 mV s^{-1} in cycle stability measurements. In-situ optical transmission spectra as a function of the applied potential were recorded by the ASD LabSpec 4 VIS/NIR spectrometer. Measurements of the transmittance at specified wavelengths (633 and 1200 nm) in real time, on the other hand, were performed by a AvaSpec-UV/VIS/NIR spectrometer. The transmittance of the ITO glass in the electrolyte was used as the baseline. All potentials were quoted with respect to a Li^+/Li reference. Switching time is defined as the time required to reach 90% of the full modulation in the specified potential range. Coloration efficiency (CE)

was calculated from the formula: $CE = \Delta OD/\Delta Q = \log(T_b/T_c)/\Delta Q$, where ΔQ is the injected charge, T_b and T_c are the transmittance in the bleached and colored states at the specified wavelength respectively.

Supplementary Figures and Table

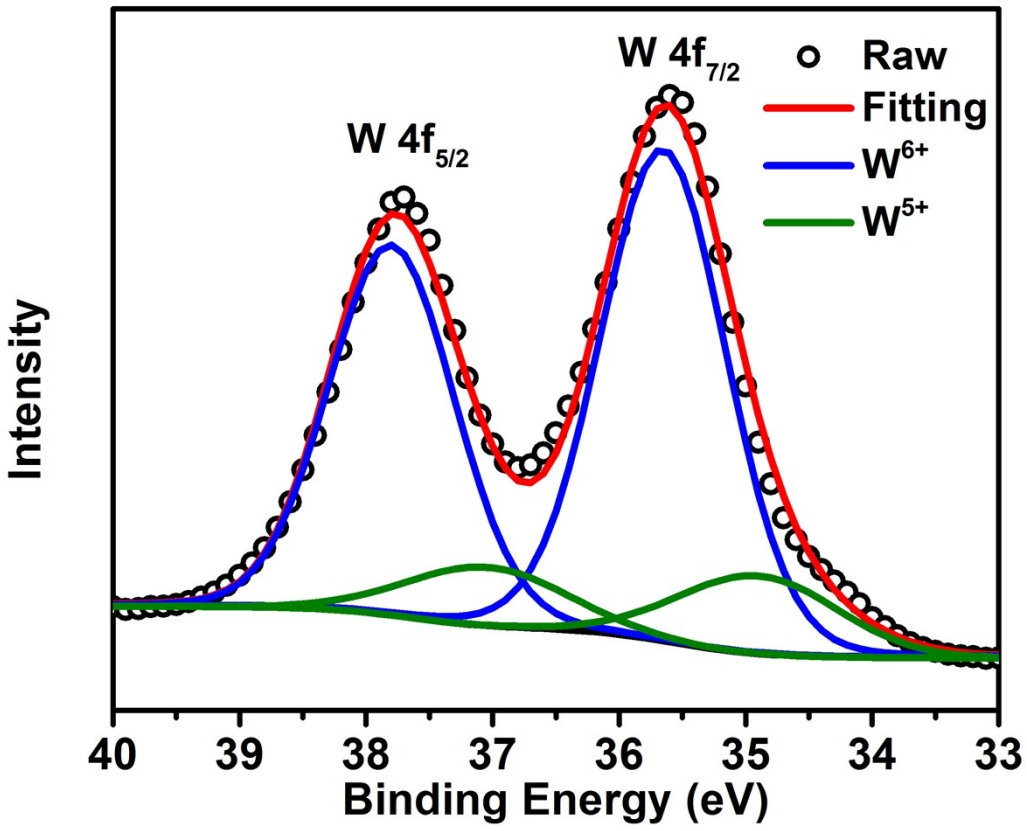

Fig. S1 W 4f XPS spectrum of m-WO_{3-x} NW film.

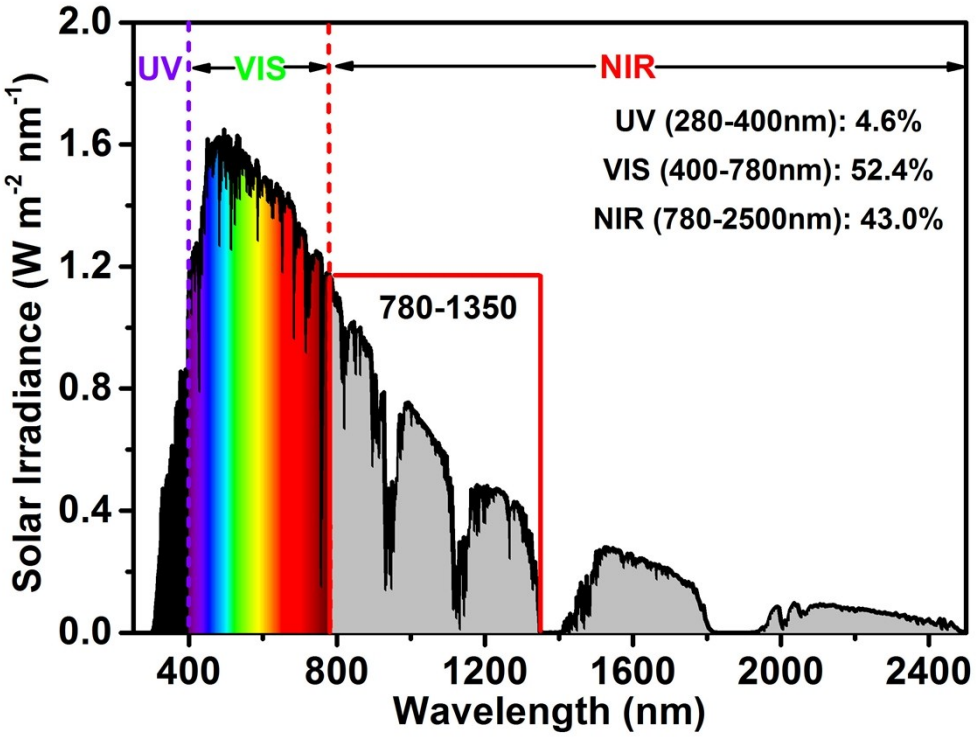

Fig. S2 The solar irradiance spectrum at air mass 1.5.

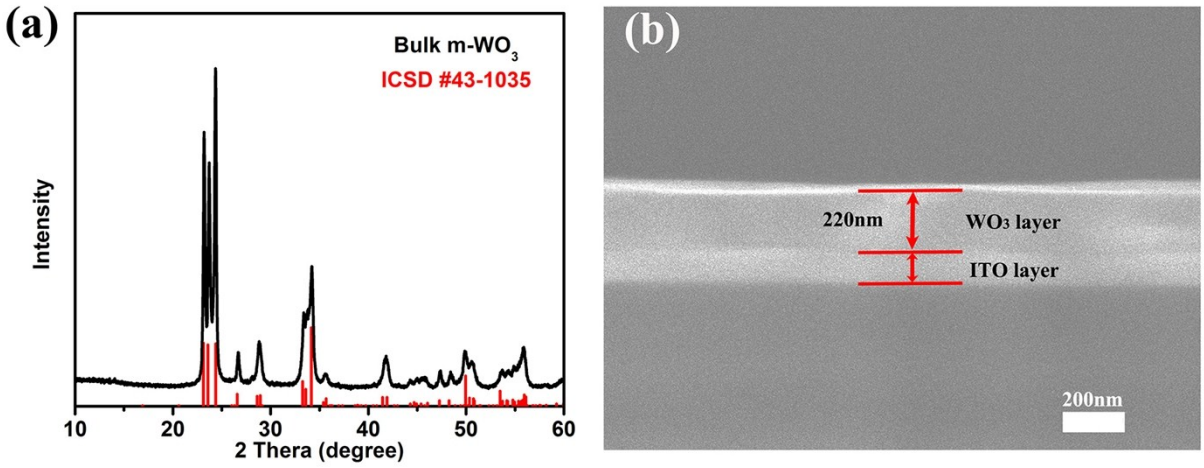

Fig. S3 (a) XRD pattern and (b) cross-section SEM image of a bulk monoclinic WO_3 (bulk m-WO_3) film (~220 nm in thickness).

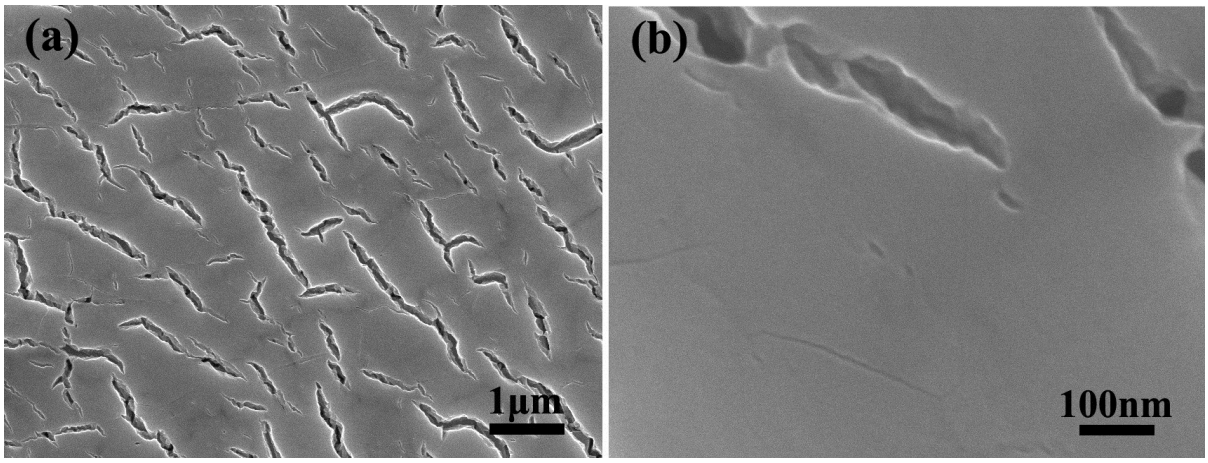

Fig. S4 (a, b) SEM images of bulk m-WO_3 film.

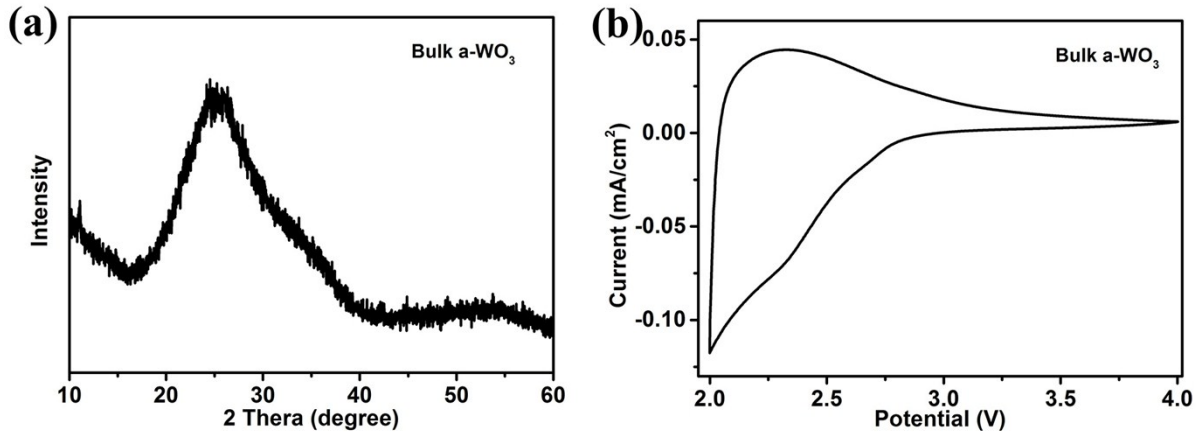

Fig. S5 (a) XRD pattern and (b) CV of a bulk amorphous WO_3 (bulk a-WO_3) film at 2 mV s^{-1}.

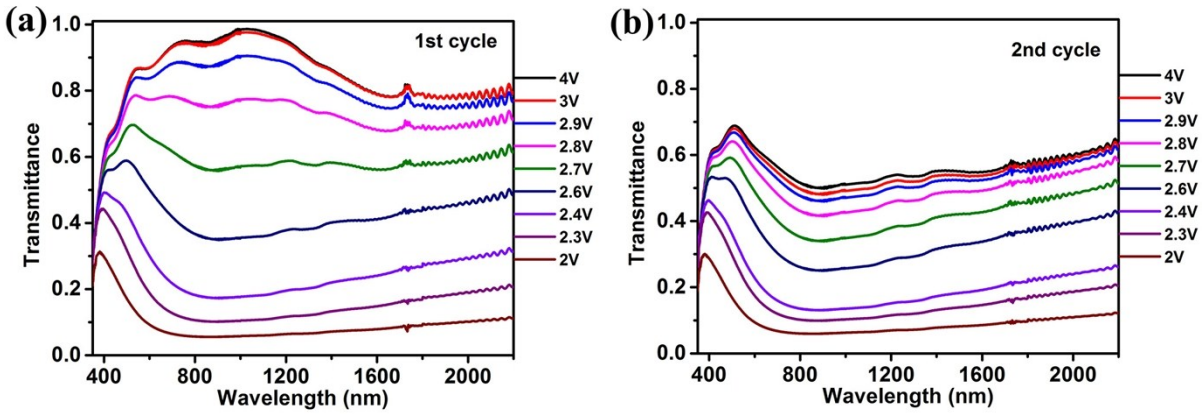

Fig. S6 First cycle (a) and second cycle (b) optical transmittance spectra of bulk amorphous WO_3 film between 4-2 V (vs Li^+/Li).

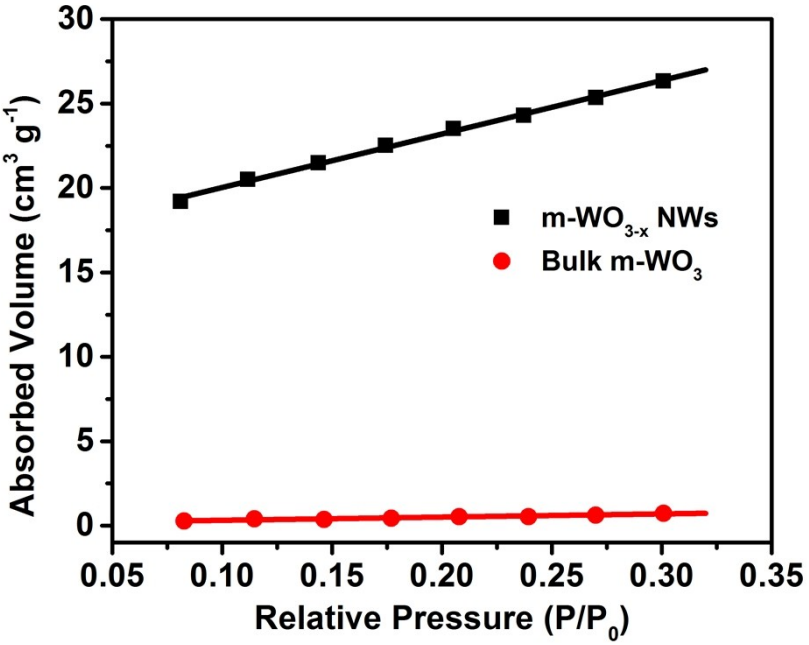

Fig. S7 The N_2 adsorption isotherm of m-WO_{3-x} NWs and bulk m-WO_3.

Table S1. Comparison of electrochromic performance (optical modulation, switching time, coloration efficiency and cycle stability) of available dual-band electrochromic materials. t_c and t_b are respectively, the coloration time and the bleaching time. CE is coloration efficiency. N/A indicates data is not available.

Material	**ΔT_{633nm}**	**ΔT_{800nm}**	**ΔT_{1200nm}**	**ΔT_{1600nm}**	**t_c/t_b (s)**	**CE ($cm^2\ C^{-1}$)**	**Cycle stability**
ITO-NbO_x[1]	~35%	~25%	~17%	~45%	N/A	30 ±4 at λ=500nm	2000 cycles (4% capacity loss)
WO_{3-x}-NbO_x[2]	~80%	~85%	~85%	~75%	N/A	N/A	2000 cycles (5.7% capacity loss)
PMe_2T_2-ITO[3]	~25%	~45%	~40%	~35%	68/19 at λ=700nm	N/A	200 cycles (15-20% capacity loss)
ITO-NbO_x[4]	~40%	~28%	~38%	~66%	N/A	N/A	1000 cycles (5% capacity loss)
Nb-TiO_2[5]	~76%	~68%	~60%	~63%	105/~10 at λ=500nm	N/A	200 cycles
$W_{18}O_{49}$/PB[6]	71.2%	~78%	~50%	64.8%	2.4/4.2 at λ=633nm	N/A	100 cycles (30% capacity loss)
WO_x-NbO_x[7]	~80%	~78%	~65%	~55%	N/A	N/A	2000 cycles
m-WO_{3-x} NWs Our work	91.7%	92.7%	94.6%	87.3%	21/85 at λ=633nm 22/75 at λ=1200nm	101.7 at λ=633nm 184.3 at λ=1200nm	1000 cycles (20.0% capacity loss, 8.3% optical loss at 633nm)

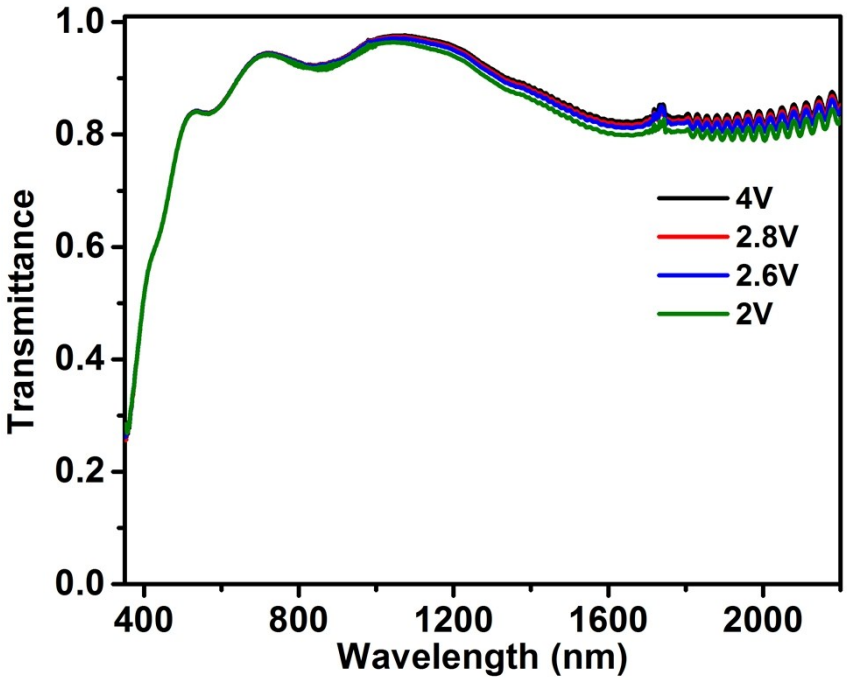

Fig. S8 Optical transmittance spectra of bulk m-WO_3 in the 4-2 V (vs Li^+/Li) potential window. Electrolyte: 0.1 M TBA-TFSI in PC.

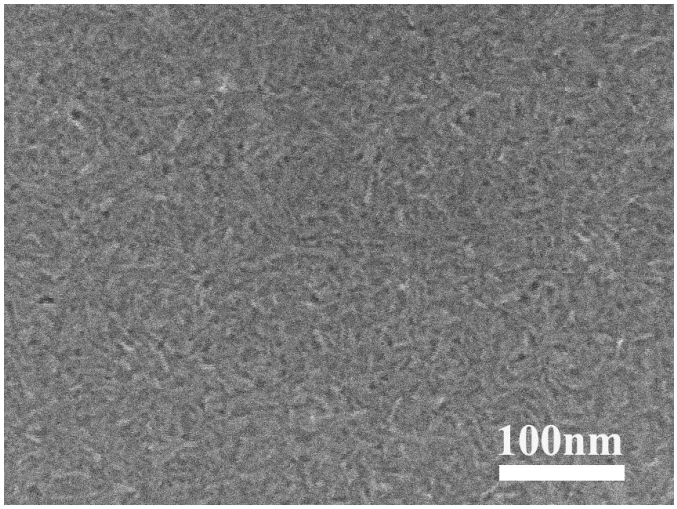

Fig. S9 .SEM image of a m-WO_{3-x} NW film after 1000 cycles.

References

1. A. Llordés, G. Garcia, J. Gazquez and D. J. Milliron, *Nature*, 2013, **500**, 323.
2. J. Kim, G. K. Ong, Y. Wang, G. LeBlanc, T. E. Williams, T. M. Mattox, B. A. Helms and D. J. Milliron, *Nano Lett.*, 2015, **15**, 5574-5579.
3. C. J. Barile, D. J. Slotcavage and M. D. McGehee, *Chem. Mater.*, 2016, **28**, 1439-1445.
4. A. Llordes, Y. Wang, A. Fernandez-Martinez, P. Xiao, T. Lee, A. Poulain, O. Zandi, C. A. Saez Cabezas, G. Henkelman and D. J. Milliron, *Nat. Mater.*, 2016, **15**, 1267-1273.
5. M. Barawi, L. De Trizio, R. Giannuzzi, G. Veramonti, L. Manna and M. Manca, *ACS Nano*, 2017, **11**, 3576-3584.
6. Z. Wang, Q. Zhang, S. Cong, Z. Chen, J. Zhao, M. Yang, Z. Zheng, S. Zeng, X. Yang, F. Geng and Z. Zhao, *Adv. Optical Mater.*, 2017, **5**, 1700194.
7. S. Heo, J. Kim, G. K. Ong and D. J. Milliron, *Nano Lett.*, 2017, **17**, 5756-5761.